Monolithic Waveguide Coupled Cavity Lasers and Modulators Fabricated by Impurity Induced Disordering

ROBERT L. THORNTON, MEMBER, IEEE, WILLIAM J. MOSBY, AND THOMAS L. PAOLI, FELLOW, IEEE

Abstract—**In this paper we describe results on AlGaAs integrated optoelectronic devices consisting of combinations of buried passive waveguide regions with active multiple quantum well gain regions. We have developed a technique for accomplishing this integration in which the waveguide regions have greatly reduced propagation loss at the gain wavelength of the active media. We have incorporated sections of waveguide into laser cavities, and the resulting low (7–11 mA) threshold currents and weak dependence of threshold current on waveguide length confirm the reduced loss and waveguiding nature of the waveguide regions. We have used these structures to monolithically couple laser amplifiers to electroabsorption modulators. Among our results on these devices are electroabsorption modulators with contrast ratios of 23:1 and monolithic *Q*-switch operation resulting in pulse widths of less than 200 ps. The relative simplicity with which these structures are fabricated via impurity induced disordering techniques promises to result in a major impact on practical systems for monolithic integration.**

Introduction

THE INTEGRATION of active laser devices with transparent waveguides is an important capability for the realization of III-V advanced optoelectronics. There has been much work done on the fabrication of ridge waveguides on GaAs for long wavelength ($1.1^{+}\mu m$) optical modulation [1], [2]. For the purpose of monolithic integration, however, it is desirable to have the waveguide transparent at the emission wavelength of a laser fabricated on the same substrate. Coupling of an integrated laser to a transparent waveguide has been successfully achieved in InGaAsP quaternary laser material by having two parallel waveguides couple evanescently [3]. However, since the laser and waveguide are not coaxial in this case, there is considerable scattering (reflection) at the transition region between the laser and waveguide. Zn diffusion has also been succesfully used to shift the wavelength of an InGaAsP active region such that low loss waveguiding can be achieved [4], [5]. Impurity induced disordering (IID) has been used to construct buried heterostructure lasers [6], [7], [8], and the passive waveguiding properties of disordered superlattice structure waveguides have been studied [9], [10]. In this paper we present results on buried two-dimensional waveguides fabricated by IID and their application to the construction of a monolithic laser with an integral cavity absorption modulator. The loss in these waveguides is sufficiently low to eliminate the need for etching and regrowth in order to monolithically integrate several optical components. We show that very efficient optical coupling between the gain region, waveguide and modulator can be achieved, resulting in efficient laser operation as well as strong modulation with on-off ratios in excess of 23:1. In addition to 8-ns pulsed operation of this device, we have also operated this device in a Q-switched mode, obtaining a 28 mw peak pulse with a pulse width under 200 ps.

Manuscript received September 15, 1987; revised January 8, 1988.

The authors are with the Xerox Palo Alto Research Center, Palo Alto, CA 94304.

IEEE Log Number 8820209.

Device Fabrication

The devices described in this study were fabricated from material grown by the metalorganic chemical vapor deposition (MO-CVD) technique. The structures are grown on n-type GaAs substrates. The as-grown epitaxial layer structure for these devices is shown in Table I. The structure is a multiple quantum well structure that is a proven design for the fabrication of high power and high efficiency buried heterostructure lasers. Once the epitaxial layers are grown, buried heterostructure regions are patterned using the silicon impurity induced disordering (Si-IID) process previously described [11], [12]. The process involves the deposition of a Si_3N_4 stripe pattern to serve as a mask for a silicon diffusion, followed by the deposition of a Si/Si_3N_4 bilayer film to serve as a source for the silicon diffusion. A silicon diffusion is then performed at 850°C for 8 h, allowing the Si diffusion to penetrate into the crystal beyond the plane of the active region. The high silicon concentration in the diffused regions promotes an enhanced rate of interdiffusion of the discrete layers in the multilayered epitaxial structure, resulting in the formation of a buried heterostructure active region. Fig. 1(a) shows the cross section of the Si_3N_4 mask and resulting diffusion profile for defining the buried heterostructure active region.

The formation of the waveguide regions is a relatively minor variation on the technique for forming the buried heterostructure gain region. In Fig. 1(b) we show the basic technique by which the active region of the laser structure

0733-8724/88/0600-0786$01.00

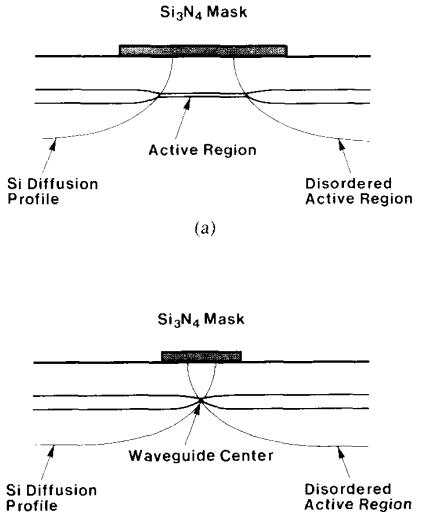

Fig. 1. Schematic diagram of the diffusion masking and diffusion profiles in the (a) optically pumped and (b) transparent waveguide sections of the composite cavity laser.

TABLE I
EPITAXIAL LAYER STRUCTURE GROWN FOR DEVICE FABRICATION

Layer #	Thickness	Al Mole Fraction	Doping	Function
1	0.5μm	0.0	Se, 1.5×10^{18}	Buffer Layer
2	0.5μm	0.2	Se, 1.5×10^{18}	Buffer Layer
3	1.4μm	0.4	Se, 1.0×10^{18}	Lower Cladding Layer
4, 6, 8, 10	20nm	0.01	——	Active Region Wells
5, 7, 9	10nm	0.20	——	Active Region Barriers
11	0.9μm	0.4	Mg, 2.0×10^{18}	Upper Cladding Layer
12	0.1μm	0.0	Mg, 5.0×10^{18}	Contacting Layer

is converted into a transparent waveguide region. We have demonstrated a similar principle in the formation of a one dimensional waveguide for a high power array laser [13]. For the waveguide region formation the lateral Si diffusions from both sides of the Si_3N_4 are allowed to merge and pinch off the active region stripe. This results in the introduction of some Al into the core of the waveguide by the effect of enhanced interdiffusion from the cladding layers, and thereby an increase in the bandgap of the material directly beneath the masking stripe, in the plane of the as-grown active region. The interdiffusion there will not be as complete as in the areas where there is no nitride, however, because it takes longer for the Si diffusion front to extend beneath the center of the nitride stripe. The less extensive interdiffusion beneath the stripe results in a local maximum in the gallium composition of the alloy at a point directly beneath the center of the nitride stripe. As a result, there is a maximum in refractive index at this point, yielding a two dimensional waveguide that is coaxial to the original active region. This process is depicted

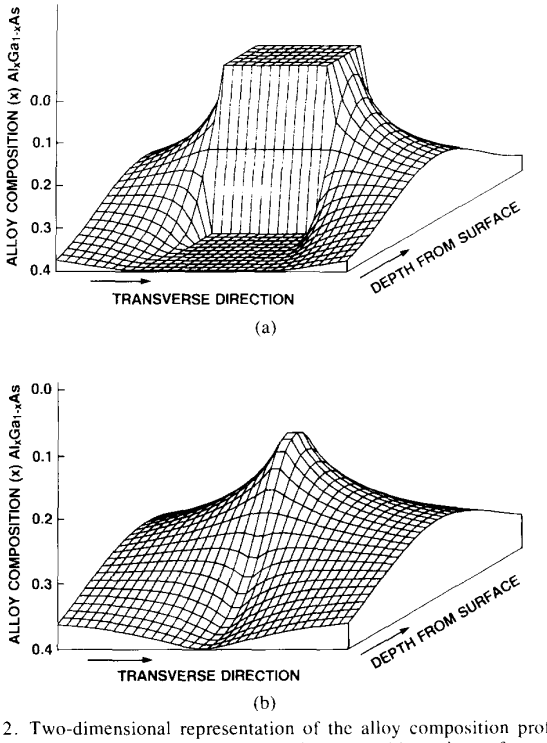

Fig. 2. Two-dimensional representation of the alloy composition profile in the (a) buried heterostructure and (b) waveguide regions of a composite cavity laser.

in the three dimensional plots of Fig. 2, where the two dimensional alloy composition is plotted schematically in the two areas corresponding to the active region and the waveguide region, for the case of an initially uniform GaAs layer sandwiched between two $Al_{.4}Ga_{.6}As$ layers. The peaks in both graphs correspond to maxima in Ga composition, and therefore maxima in refractive index. The waveguiding nature of these structures is therefore apparent. In the passive waveguide region, the local peak in Ga composition will be a sensitive function of the total time for the diffusion, but could conceivably be varied controllably in the range from 20-percent aluminum to 35-percent aluminum. The strength and modal properties of the waveguide would vary in relation to the two dimensional composition profile generated. The two dimensional profile is the result of the solution of a two dimensional diffusion problem with time dependent boundary conditions, and is therefore very complicated. Numerical solution would be the most effective approach to solving for the eigenmodes of the resulting waveguide.

In Fig. 3 we show SEM crossections corresponding to the two regions depicted schematically in Fig. 1. The crossections in Fig. 3 have been heavily stained in a common *AB* etch procedure [14] to enhance the contrast due to the varying aluminum composition. The pinched off waveguide in Fig. 3(b) does not retain any of the fine quantum well structure which is still present in the nondisordered active section of the device in Fig. 3(a). The waveguide is therefore low in absorption at the emission

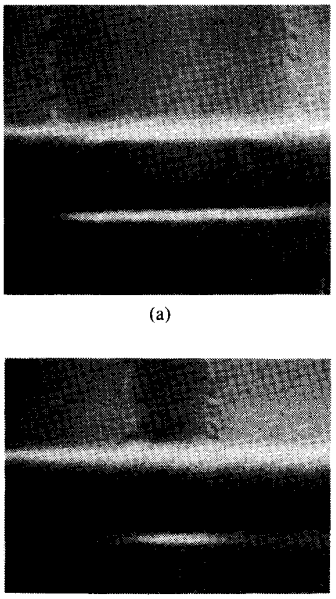

(a)

(b)

Fig. 3. SEM cross sections showing (a) the buried heterostructure laser section (actively pumped region), and (b) the transparent optical waveguide section of the composite laser cavity.

wavelength corresponding to radiative transitions in the quantum wells. Proton bombardment isolation is used to insure that current is injected only in the regions of the crystal that contain nondisordered (as-grown) active region material. Since the waveguide regions are therefore not electrically pumped, we would expect much greater absorption in these regions if they did not in fact consist entirely of material with wider bandgap than the as-grown active region.

Optical Properties of Devices

We have characterized the performance of these diffused waveguides by incorporating sections of waveguide into cavities of Si-IID buried heterostructure lasers. The results are shown in Fig. 4, where we show the lasing characteristics of these devices as a function of the length of the waveguide region in the laser cavity. We see only a slight decrease in slope efficiency and increase in threshold for cavity waveguide region lengths as long as 60 μm, or 27 percent of the total cavity length. The increase in threshold current will be the result of two effects; scattering loss at the waveguide–active region interface and propagation loss in the waveguide region. The scattering loss will be a result of the different modal widths of the two waveguides [15]. By characterizing the threshold variation with waveguide length, we have developed an estimate of the magnitudes of both the scattering loss and the propagation loss in these composite cavity structures. By assuming that the gain coefficient in the pumped regions has two components, a constant loss component and a gain component that is proportional to the current density in the device [16], we can write

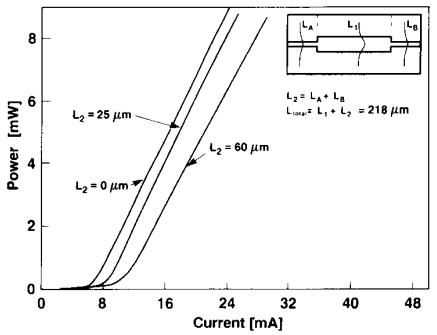

Fig. 4. Pulsed power versus current characteristics for the window lasers with two dimensional waveguiding, showing the minimal effect of increasing the length of unpumped region in the laser cavity.

$$\alpha = \alpha_1 + BI_{th}/L_1 W \tag{1}$$

where $J = I_{th}/L_1 W$ is the current density in the device at threshold current I_{th}, W is the width of the active region stripe, B is the linear current/gain coefficient, and L_1 is the length of the actively pumped section of the device. Making this assumption, we can write the laser oscillation condition in the following manner:

$$+2\alpha_1 L_1 - 2\alpha_2 L_2 + 2N(\ln S) + 2BI_{th}/W = -\ln (R_1 R_2) \tag{2}$$

where α_2 is the propagation loss in the waveguide region, L_2 is the waveguide region length, S is the fractional power remaining in the waveguide after scattering at a laser/waveguide transition, N is the number of laser/waveguide transitions in a device, and R_1, R_2 are the reflectivities of the two facets. We have assumed that the lasing mode is determined by the reflections from the cleaved facets, even though there will be some back reflection at the waveguide-active region transition. This equation contains four unknown quantities α_1, α_2, S, and B. The active region propagation loss α_1 is reduced from the intrinsic loss in a uniform GaAs region by a factor of Γ, the confinement factor which represents the fraction of the waveguided mode which overlaps the active region wells which provide optical gain and absorption. Since in the active region the absorption is dominated by band to band absorption in the quantum wells, the parameter Γ is well defined, and has a value of 0.25 for the structure described in Table I. The confinement factor is not a well defined parameter for the waveguide region, however, since the alloy composition profile varies gradually across the guided mode profile. The absorption, which we attribute to the presence of free carriers in the waveguide region, is therefore, not dominated by any discrete alloy composition layer in the waveguide region. Since the magnitude of the free carrier absorption is not a strong function of the alloy composition, we conclude that the absorption is uniformly distributed over the entire waveguide crossection, and therefore the relevant confinement factor parameter in this region is close to unity.

TABLE II
MEASURED CHARACTERISTICS AND GEOMETRY OF FOUR DEVICES USED TO EXTRACT THE DEVICE PARAMETERS DEFINED IN (2)

Active region Length (L_1)	Waveguide Region Length (L_2)	Threshold Current	Number of Scattering Centers	Mirror Losses -ln (R_1R_2)
218.4μm	0.0μm	6.8mA	0	1.83
193.2μm	25.2μm	9.0mA	2	1.83
266.0μm	94.1μm	9.5mA	3	1.83
157.8μm	60.6μm	10.5mA	2	1.83
$\alpha_1 = 16.9cm^{-1}$	$\alpha_2 = 17.1cm^{-1}$	$B = 1.6x10^{-5}$ cm/ma	$S = .9556$	

We have measured four laser devices with waveguide and gain sections of varying lengths in order to solve for the four unknown quantities in (2). The relevant quantities measured for the four devices used are summarized in Table II, along with the values of the various parameters calculated using this data. We have solved for estimates of the scattering loss to be in the range of $L_s = 1 - S \approx 4.5$ percent, and for the waveguide propagation loss to be on the order of $\alpha_2 \approx 17\ cm^{-1}$. The propagation loss is of an appropriate magnitude to be consistent with free carrier absorption in the $\approx 7 \times 10^{18}$ n-type disordered waveguide region, but is too low to be consistent with band-to-band absorption in an unpumped waveguide at a photon energy higher than the bandgap of the alloy composition of the waveguide. We therefore conclude that the propagation loss is indeed free carrier absorption in a wide bandgap alloy that is substantially transparent at the lasing energy. It should be noted, however, that the numbers presented here are order of magnitude estimates only, and we should allow for the possibility of significant error due to the fact that the calculations would be very sensitive to other random device imperfections in these four devices that would cause changes in their threshold currents. Although the calculated propagation losses are much higher than is commonly desired in waveguides fabricated by other means in very high purity AlGaAs, the ability to readily integrate these waveguide elements with gain elements to a large degree relaxes the demands on low propagating loss for many applications.

MODULATION PROPERTIES

By using the waveguide structure described above to connect two sections of buried heterostructure multiple quantum well (MQW) active region, we have realized a laser structure that has a monolithically integrated modulator. Functionally very similar structures have been fabricated in InGaAsP material using a sophisticated two step growth process [17] or by selective Zn diffusion [4], [5]. The structure for this laser is shown in Fig. 5. The key distinction between the amplifier and modulator sections of the device is that the amplifier section is the longer of the two. Separate contacting of the two regions is achieved by a photolithographic liftoff process applied to the Cr–Au metallization. Due to the optical waveguide coupling, very high electrical isolation of 14 MΩ is achieved between the modulator and the amplifier sections of the device.

Under proper biasing conditions, these devices exhibit very distinct nonlinear effects. CW light versus current characteristics for a typical device are shown in Fig. 6. Due to the low threshold currents achievable by Si-IID, these devices readily operate CW with the junction side up. This greatly simplifies electrical contacting to the device for driving the two sections independently. The resulting L-I characteristics clearly exhibit some of the highly nonlinear features present in these devices. The curve labeled "*a*" in this figure shows the L-I characteristics for this device with both sections driven in parallel. The device exhibits a very steep slope to its initial turn on, and a bistable region with a hysteresis loop 3 mA wide. When the modulator section current is held constant and the amplifier section is varied, as in curve "*b*" of Fig. 6, the abrupt turn-on region remains, but the hysteresis loop is no longer apparent. These hysteresis and abrupt turn on effects have been widely observed in laser structures with non-uniform pumping along the cavity length due to segmented contacts [18], [19].

We have studied the modulation characteristics of these devices, and have found that there are two distinct regions of operation of the device, as shown in Fig. 7. In this figure we have taken pulsed L-I curves from the amplifier output facet with a 700-ns pulsewidth. Each curve corresponds to a constant value of the dc current or voltage on the modulator section. For the device described in this experiment, the lengths of the amplifier, waveguide, and modulator sections were 233, 50, and 47 μm, respectively. If the modulator section is sufficiently forward biased to conduct significant current, the modulation will be a result of changes in the stimulated emission gain in the modulator section due to the changes in the carrier density in that region. This regime begins when the forward voltage reaches the turn-on voltage above which the modulator diode conducts more than a few tens of microamperes of current. In Fig. 7 this initial curve is represented by 0 mA of current at 1.33 V of applied bias. (The 0-mA curve actually corresponds to a few tens of microamperes of current.) Further increments of modulator current result in incremental increases in the optical output. We refer to this region as the gain modulation region of the device. This mode of operation is very similar in dynamics to the modulation of a semiconductor laser biased above threshold. These curves also exhibit the very steep slopes in their L-I characteristics as a result of nonuniform pumping of the cavity.

By decreasing the applied modulator voltage below the value required for gain, very strong absorption effects become evident, resulting in a very strong dependence of the laser threshold on the value of the modulator voltage. The modulation mechanism in this region is electroabsorption in the multiple quantum well active region of the as-grown laser structure. Due to the presence of the p-n junction at the MQW active region in the modulator section, there exists an electric field across the MQW even at zero bias. Given the doping levels in the cladding layers of the epitaxial structure, the magnitude of the built in

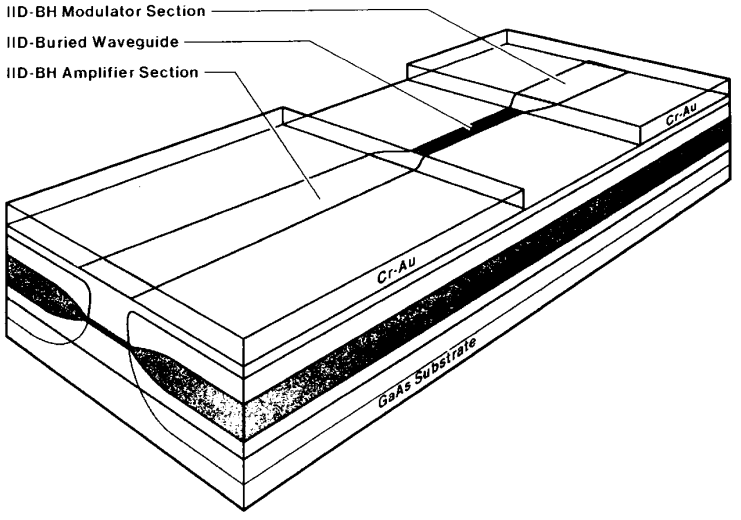

Fig. 5. Schematic diagram representing the laser diode with monolithically integrated modulator.

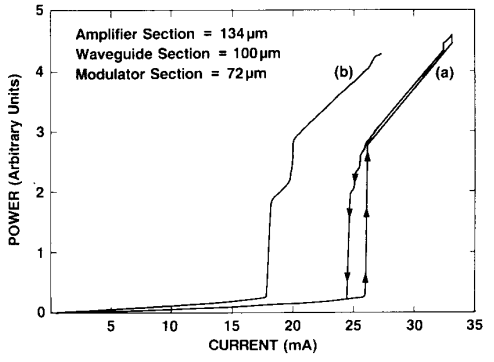

Fig. 6. CW light versus current curves for a laser modulator combination exhibiting hysteresis in its light output characteristic.

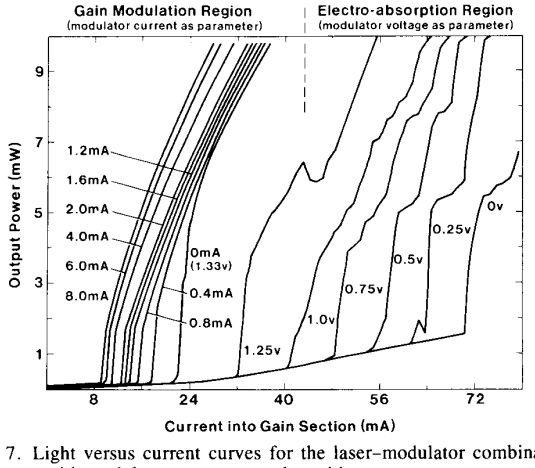

Fig. 7. Light versus current curves for the laser–modulator combination with modulator current or voltage bias as a parameter.

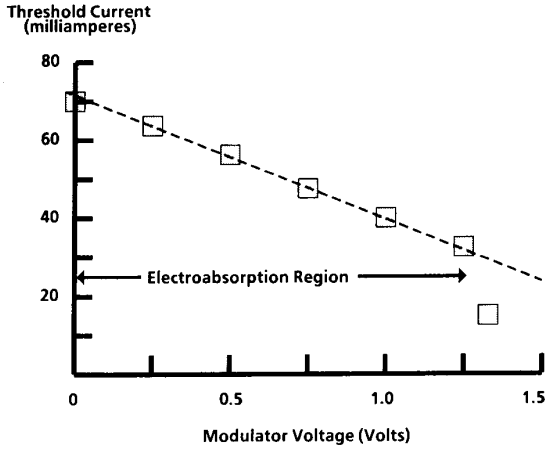

Fig. 8. Threshold current as a function of modulator section voltage bias, demonstrating the high degree of device linearity in the electroabsorption region.

electric field will be on the order of 2.0×10^5 V/cm. This field results in significant electroabsorption in this device even at zero applied external bias, i.e., the device is "normally off" as opposed to the "normally on" operation that is achieved when the internal electric field is zero when the external applied voltage is zero, as is usually the goal in this type of modulator structure [4], [5], [17], [20]. As a forward bias is applied to the junction, the magnitude of the built-in electric field is decreased, thereby shifting the absorption band edge to shorter wavelength and reducing the magnitude of the absorption at the maximum gain wavelength of the amplifier section. We therefore observe a decrease in lasing threshold as the positive applied voltage is increased.

These devices exhibit a very strong dependence of threshold current on modulator applied bias. In Fig. 8 we plot the device threshold current as a function of the voltage applied to the modulator section. We have achieved a threshold current ratio of 2.2 for a control voltage swing of 1.25 V. This modulation rate is a factor of 2.6 greater

than that reported in previous devices of this type [5], [20].

As a result of the strong electroabsorption generated by the built in field, we are able to bias the amplifier section at currents well above the on-state lasing value without observing lasing. This allows a high ratio to be achieved between the on and off states of the modulator with a very small voltage swing on the modulator. For example, with a dc bias of 31 mA on the amplifier section, the on-off ratio is easily in excess of 23 : 1, or 13.6 dB, with an applied modulator voltage swing of only 1.35 V, and at less than 1 mA of current. We therefore conclude that utilizing these modulator structures in a normally off configuration that takes advantage of the built-in electric field is an effective means for achieving high modulation efficiencies in these structures.

Device Transient Response

The modulator-amplifier combination should in principle provide for improved modulation relative to direct modulation of the laser due to the short time scale associated with the electroabsorption effect, the lower capacitance of the short modulator section relative to the total length of the cavity and the very high absorption obtained when the modulator section has no applied voltage. One major advantage of this structure is that it allows a convenient way of realizing very long lengths of electroabsorption, so that the modulation rate as a function of applied voltage can be very large. This facilitates the realization of faster modulation rates by reducing the voltage swing required for the modulator drive circuitry. It should be pointed out, however, that these structures have not yet been optimized to reduce parasitic components, mainly contact metalization and p-n junction capacitance, which would slow the modulation speed of the device.

To evaluate the modulation properties, we have observed the operation of this device under high speed pulsed operation. By biasing the laser section to a constant dc current and applying a several nanosecond pulse to the modulator section, we are able to generate a fast output pulse from the device. Fig. 9(a) shows the output pulse for a trigger pulse of 8-ns duration and rise and fall times of 2–3 ns. The output response pulse is shortened due to the delayed turn-on effects that have been previously observed in these devices [18], but it is important to note that the output pulse has an initial risetime which is faster than the risetime of the driving pulse, and consists of a large amplitude initial Q-switching pulse, followed by a relaxation oscillation that brings the amplitude of the pulse down to its steady state level. In Fig. 9(b) we have adjusted the amplitude and width of the modulator pulse such that only the large Q-switched pulse is observed. As a result, we are able to obtain a pulse with a <200 ps FWHM. The actual pulse width is significantly narrower than 200 ps, as the photodetector used had a FWHM of 185 ps. The observed peak output power in this pulse is 25 mW. This number is also an underestimate due to the insufficiently fast photodetector response. These results indicate that the response times in the modulator are fast, although more detailed high speed measurements and device optimization will be necessary to reach the limits of modulation rates in these devices.

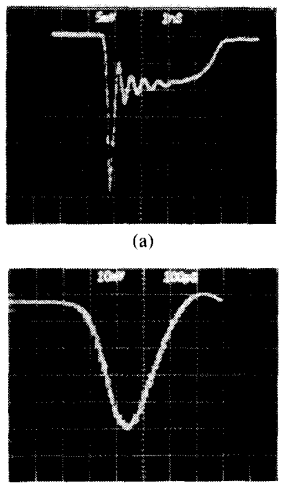

(a)

(b)

Fig. 9. Pulse output with a CW bias current on the gain port and (a) an 8-ns 3-mA current pulse on the modulator port (31-mA bias) and (b) an 8-ns 0.5-mA current pulse on the modulator port (33-mA bias).

Conclusions

In conclusion, we report results on low-loss optical waveguides in the AlGaAs alloy system fabricated by impurity induced disordering. These waveguides are monolithic and planar, and are subsurface structures that are easily made coplanar and co-axial with buried regions of gain (such as the active region of a semiconductor laser). They exhibit relatively low propagation loss at the wavelength at which such an active region would emit radiation. In addition, we have successfully coupled these waveguide regions to active gain elements, and confirmed that the waveguide performance allows extended regions of unpumped cavity without a major increase in lasing threshold or decrease in device efficiency. We have constructed a composite laser with an internal cavity modulator, and observed operation of the modulator section in both a gain modulation and an electroabsorption modulation mode. Utilizing the electroabsorption mode we have modulated the device with a contrast ratio of 23 : 1 with an applied voltage swing between 0 and 1.35 V. By using the very strong electroabsorption in the modulator, we have operated the device in a Q-switched mode and obtained pulse widths of well under 200 ps.

Acknowledgment

The authors gratefully acknowledge helpful technical discussions with J. Epler, and the technical assistance of H. Chung, R. Donaldson, F. Endicott, S. Nelson, D. Taylor, T. Tjoe, and D. Treat.

REFERENCES

[1] H. Inoue, K. Hiruma, K. Ishida, T. Asai, and H. Matsumura, "Low loss GaAs optical waveguide," *J. Lightwave Technol.*, vol. LT-3, pp. 1270-1276, 1985.

[2] E. Kapon and R. Bhat, "Low-loss single-mode GaAs/AlGaAs optical waveguides grown by organometallic vapor phase epitaxy," *Appl. Phys. Lett.*, vol. 50, pp. 1628-1630, 1987.

[3] N. K. Dutta, T. Cella, A. B. Piccirilli, and R. L. Brown, "Integrated external cavity lasers," in *Conf. Lasers and Electrooptics Tech. Dig. Series 1987*, vol. 14. Washington, DC: Optical Society of America, 1987, p. 22.

[4] D. Z. Tsang, J. N. Walpole, S. H. Groves, J. J. Hsieh, and J. P. Donnelly, "Intracavity loss modulation of GaInAsP diode lasers," *Appl. Phys. Lett.*, vol. 38, no. 3, pp. 120-123, 1981.

[5] D. Z. Tsang, J. N. Walpole, Z. L. Liau, S. H. Groves, and V. Diadiuk, "*Q*-Switching of low-threshold buried-heterostructure diode lasers at 10 GHz," *Appl. Phys. Lett.*, vol. 45, no. 3, pp. 204-206, 1984.

[6] K. Meehan, P. Gavrilovic, N. Holonyak, Jr., R. D. Burnham, and R. L. Thornton, "Stripe geometry $Al_xGa_{1-x}As$-GaAs quantum well heterostructure lasers defined by Si diffusion and disordering," *Appl. Phys. Lett.*, vol. 46, pp. 75-77, 1985.

[7] R. L. Thornton, R. D. Burnham, T. L. Paoli, N. Holonyak, Jr., and D. G. Deppe, "Low threshold planar buried heterostructure lasers fabricated by impurity induced disordering," *Appl. Phys. Lett.*, vol. 47, no. 12, pp. 1239-1241, 1985.

[8] D. G. Deppe, K. C. Hsieh, N. Holonyak, Jr., R. D. Burnham, and R. L. Thornton, "Low threshold disorder-defined buried heterostructure $Al_xGa_{1-x}As$-GaAs quantum well lasers," *J. Appl. Phys.*, vol. 58, pp. 4515-4520, 1985.

[9] F. Julien, P. D. Swanson, M. A. Emanuel, D. G. Deppe, T. A. DeTemple, J. J. Coleman, and N. Holonyak, "Impurity-induced disorder-delineated optical waveguides in GaAs-AlGaAs superlattices," *Appl. Phys. Lett.*, vol. 50, pp. 866-868, 1987.

[10] E. Kapon, N. G. Stoffel, E. A. Dobisz, and R. Bhat, "GaAs/AlGaAs channel waveguides made by impurity-induced superlattice disordering," in *Conf. Lasers and Electrooptics Tech. Dig. Series 1987*, vol. 14. Washington, DC: Optical Society of America, 1987, p. 200.

[11] K. Meehan, N. Holonyak, Jr., J. M. Brown, M. A. Nixon, P. Gavrilovic, and R. D. Burnham, "Disorder of an $Al_xGa_{1-x}As$-GaAs superlattice by donor diffusion," *Appl. Phys. Lett.*, vol. 45, pp. 549-551, 1984.

[12] R. L. Thornton, R. D. Burnham, T. L. Paoli, N. Holonyak, Jr., and D. G. Deppe, "Optoelectronic device structures fabricated by impurity induced disordering," *J. Crystal Growth 77*, pp. 621-628, 1986.

[13] R. L. Thornton, D. F. Welch, R. D. Burnham, T. L. Paoli, and P. S. Cross, "High power (2.1-W) 10-stripe AlGaAs laser arrays with Si disordered facet windows," *Appl. Phys. Lett.*, vol. 49, no. 23, pp. 1572-1574, 1986.

[14] G. H. Olsen and M. Ettenberg, *J. Appl. Phys.*, vol. 45, p. 5112, 1974.

[15] H. Kogelnik, Ed., *Proc. Symp. Quasioptics*. Brooklyn, NY: Polytechnic, 1964, p. 333.

[16] B. W. Hakki and T. L. Paoli, "Gain spectra in double heterostructure injection lasers," *J. Appl. Phys.*, vol. 46, p. 1299, 1975.

[17] Y. Kawamura, K. Wakita, Y. Itaya, Y. Yoshikuni, and H. Asahi, "Monolithic integration of InGaAsP/InP DFB lasers and InGaAs/InAlAs MGW optical modulators," *Electron. Lett.*, vol. 22, pp. 242-243, 1986.

[18] C. Harder, K. Y. Lau, and A. Yariv, "Bistability and pulsations in semiconductor lasers with inhomogeneous current injection," *IEEE J. Quantum Electron.*, vol. QE-18, no. 9, pp. 1351-1361, 1982.

[19] J. K. Carney and C. G. Fonstad, "Double-heterojunction laser diodes with multiply segmented contacts," *Appl. Phys. Lett.*, vol. 38, no. 5, pp. 303-305, 1981.

[20] Y. Arakawa, A. Larsson, J. Paslaski, and A. Yariv, "Active *Q* switching in a GaAs/AlGaAs multiquantum well laser with an intracavity monolithic loss modulator," *Appl. Phys. Lett.*, vol. 48, no. 9, pp. 561-563, 1986.

*

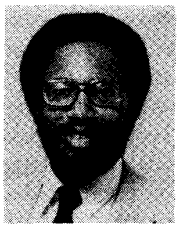

Robert L. Thornton (M'85) was born in Washington, DC, on June 29, 1955. He received a National Achievement Scholarship to attend California Institute of Technology, from which he received the B.S. degree in electrical engineering in 1977. He was the recipient of a Bell Telephone Laboratories Fellowship to attend Graduate School at Stanford University, where he earned the M.S. and Ph.D. degrees in applied physics in 1979 and 1983, respectively. His graduate research involved the design, construction, and analysis of nonlinear analog signal processing devices utilizing surface acoustic waves.

Since 1983 he has been a Member of Research Staff in the Integrated Optoelectronics Area at Xerox Palo Alto Research Center in Palo Alto, CA, where he is conducting research in the design and novel fabrication techniques for III-V optoelectronic device structures.

*

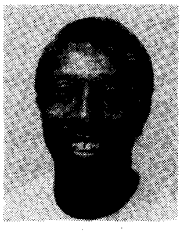

William J. Mosby was born in Boston, MA, on May 25, 1932. He received the B.S. degree from Northeastern University in Boston Massachusetts in 1952.

From 1952 to 1963 he worked at the M.I.T. Research Laboratory for Electronics on microwave components and electron devices. From 1963 to 1972 he worked in the M.I.T. Frances Bitter National Magnet Laboratory on Mossbauer spectroscopy on magnetic materials and localized magnetic moments in metals. In 1972 he joined Xerox Corporation's Palo Alto Research Center, where he has been involved in Raman Spectroscopy of amorphous materials and UHV techniques for thin films. His current activities involve the design and implementation of novel III-V laser structures for optoelectronic applications.

*

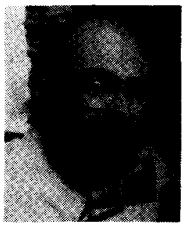

Thomas L. Paoli (S'59-M'73-SM'80-F'88) received the B.S. degree in electrical engineering and the B.A. degree from Brown University, Providence, RI, and the Ph.D. degree in applied physics from Stanford University, Stanford, CA. While attending Stanford, he was a fellow of the National Science Foundation.

He has contributed extensively to the research and development of semiconductor lasers for optical communications and other applications. From 1967 to 1981 he was a Member of the Technical Staff at Bell Laboratories, Murray Hill, NJ, and currently is Manager of the Optoelectronics Materials and Devices Area, at the Xerox Palo Alto Research Center, Palo Alto, CA. He has also held positions with the Applied Research Laboratory and the Electronic Defense Laboratories of Sylvania Electronic Systems and has been a Visiting Professor at the University of Campinas, Campinas, Brazil. He has published more than 150 papers and has been awarded 12 patents.

Dr. Paoli is a member of Phi Beta Kappa, Tau Beta Pi, Sigma Xi, and the American Physical Society.